AMERICAN SOCIETY FOR MICROBIOLOGY | Journal of Virology®

GENOME REPLICATION AND REGULATION OF VIRAL GENE EXPRESSION

Identification and Cloning of a New Western Epstein-Barr Virus Strain That Efficiently Replicates in Primary B Cells

Susanne Delecluse,[a,b,c,d] Remy Poirey,[a,b,c] Martin Zeier,[d] Paul Schnitzler,[e] Uta Behrends,[c,f,g] Ming-Han Tsai,[h] Henri-Jacques Delecluse[a,b,c]

[a]German Cancer Research Centre (DKFZ), Unit F100, Heidelberg, Germany
[b]Institut National de la Santé et de la Recherche Médicale (INSERM), Unit U1074, Heidelberg, Germany
[c]German Center for Infection Research (DZIF), Braunschweig, Germany
[d]Nierenzentrum Heidelberg, Heidelberg, Germany
[e]Center for Infectious Diseases, Virology, University Hospital Heidelberg, Heidelberg, Germany
[f]Children's Hospital Schwabing, Technische Universität München, Munich, Germany
[g]Research Unit Gene Vectors, Helmholtz Zentrum München, German Research Center for Environmental Health, Munich, Germany
[h]Institute of Microbiology and Immunology, National Yang-Ming University, Taipei, Taiwan

ABSTRACT The Epstein-Barr virus (EBV) causes human cancers, and epidemiological studies have shown that lytic replication is a risk factor for some of these tumors. This fits with the observation that EBV M81, which was isolated from a Chinese patient with nasopharyngeal carcinoma, induces potent virus production and increases the risk of genetic instability in infected B cells. To find out whether this property extends to viruses found in other parts of the world, we investigated 22 viruses isolated from Western patients. While one-third of the viruses hardly replicated, the remaining viruses showed variable levels of replication, with three isolates replicating at levels close to that of M81 in B cells. We cloned one strongly replicating virus into a bacterial artificial chromosome (BAC); the resulting recombinant virus (MSHJ) retained the properties of its nonrecombinant counterpart and showed similarities to M81, undergoing lytic replication *in vitro* and *in vivo* after 3 weeks of latency. In contrast, B cells infected with the nonreplicating Western B95-8 virus showed early but abortive replication accompanied by cytoplasmic BZLF1 expression. Sequencing confirmed that rMSHJ is a Western virus, being genetically much closer to B95-8 than to M81. Spontaneous replication in rM81- and rMSHJ-infected B cells was dependent on phosphorylated Btk and was inhibited by exposure to ibrutinib, opening the way to clinical intervention in patients with abnormal EBV replication. As rMSHJ contains the complete EBV genome and induces lytic replication in infected B cells, it is ideal to perform genetic analyses of all viral functions in Western strains and their associated diseases.

IMPORTANCE The Epstein-Barr virus (EBV) infects the majority of the world population but causes different diseases in different countries. Evidence that lytic replication, the process that leads to new virus progeny, is linked to cancer development is accumulating. Indeed, viruses such as M81 that were isolated from Far Eastern nasopharyngeal carcinomas replicate strongly in B cells. We show here that some viruses isolated from Western patients, including the MSHJ strain, share this property. Moreover, replication of both M81 and of MSHJ was sensitive to ibrutinib, a commonly used drug, thereby opening an opportunity for therapeutic intervention. Sequencing of MSHJ showed that this virus is quite distant from M81 and is much closer to nonreplicating Western viruses. We conclude that Western EBV strains are heterogeneous, with some viruses being able to replicate more strongly and therefore being potentially more pathogenic than others, and that the virus sequence information alone cannot predict this property.

Citation Delecluse S, Poirey R, Zeier M, Schnitzler P, Behrends U, Tsai M-H, Delecluse H-J. 2020. Identification and cloning of a new Western Epstein-Barr virus strain that efficiently replicates in primary B cells. J Virol 94:e01918-19. https://doi.org/10.1128/JVI.01918-19.

Editor Richard M. Longnecker, Northwestern University

Address correspondence to Ming-Han Tsai, m.tsai@ym.edu.tw, or Henri-Jacques Delecluse, h.delecluse@dkfz.de.

Received 12 November 2019
Accepted 14 February 2020
Accepted manuscript posted online 26 February 2020
Published 4 May 2020

KEYWORDS Epstein-Barr virus, lytic replication, recombinant virus

The Epstein-Barr virus (EBV) is a member of the *Gammaherpesvirinae* subfamily that causes infectious mononucleosis (IM) and malignant diseases (1). EBV is strongly B lymphotropic and is etiologically associated with B-cell lymphoproliferations, the incidence of which rises strikingly in immunosuppressed individuals (1). This population includes elderly patients and patients with acquired immune deficiency, e.g., after HIV infection or intake of immunosuppressive drugs in solid organ transplantation (SOT) or stem cell transplantation (SCT) recipients (2). The latter patients develop posttransplant lymphoproliferative disorders (PTLD). These tumors frequently express the EBV latent genes as well as EBV microRNAs (miRNAs) (1, 3).

In infected B cells, EBV classically induces a viral latency that is characterized by cell proliferation, expression of the full set of latent genes and absent or limited lytic replication, the process that leads to the production of virus progeny (1). These characteristics are easily identifiable in B cells infected with the B95-8 strain either *in vitro* or in infected humanized mice (4). B95-8 was isolated from a U.S. patient with infectious mononucleosis and is thought to be representative of the virus found in IM patients and more generally in the Western population. However, we have recently shown that the M81 virus, isolated from a Chinese patient with nasopharyngeal carcinoma (NPC), induces potent lytic replication in B cells from normal individuals, both *in vitro* and in humanized mice (4).

Epidemiological studies have identified viral lytic replication as a risk factor for the development of some EBV-associated lymphomas and carcinomas (5). High antibody titers against EBV replicative antigens are predictive of NPC several years in advance (6). Furthermore, more than 90% of EBV-positive PTLD contain cells undergoing replication and express BZLF1, the key viral transactivator that initiates EBV lytic replication, or early and late EBV lytic antigens such as early D antigen (EA-D) (7). Similar features were recorded in AIDS-associated lymphomas (8). We recently demonstrated that the EBV particles themselves can confer chromosomal instability and aneuploidy after contact with target B cells (9). This establishes a direct mechanistic link between lytic replication and cancer risk development.

In this study, we report the properties of viruses present in spontaneous cell lines generated from 13 transplant recipients and from 9 patients with IM. We cloned the genome of one of these viruses that displayed potent replication in primary B cells onto a bacterial artificial chromosome (BAC) and compared its characteristics to those of well-characterized laboratory strains.

RESULTS

Spontaneously growing EBV-transformed B cells from patients with IM or iEBVL frequently replicate the virus, although with greatly differing intensities. We first generated a panel of spontaneously growing EBV-transformed lymphoblastoid cell lines (LCL) from patients with IM or with an increased EBV load (iEBVL) in the peripheral blood (>1,000 copies/ml) (Table 1). These were established very easily from most patients from approximately 10^5 peripheral blood B cells within less than 4 weeks. We stained them shortly after establishment with antibodies specific to BZLF1 and gp350 to assess lytic replication (Fig. 1). Four weeks after seeding, 12 from 13 EBVL and 7 from 9 IM cell lines expressed the immediate early (IE) lytic protein BZLF1 and the late protein gp350 (Fig. 1). Thus, only one of the iEBVL cell lines (sLCL-10) and two of the IM cell lines (IM-7 and IM-8) were devoid of any lytic protein expression. Two-thirds of the cases contained more than 1% BZLF1-positive cells, and seven cases contained between 2 and 5.7% BZLF1-positive cells, four of which showed replication levels close to those reached by M81. However, only five EBVL and five IM cell lines expressed the late lytic protein gp350 in more than 1% of cells, and only one case reached M81 levels, in terms of combined BZLF1 and gp350 expression (Fig. 1). Here, we took into consideration only cells expressing gp350 in the entire cytoplasm and excluded cells showing patchy gp350-specific staining at the cell surface that we interpreted as B cells

TABLE 1 Characteristics of the studied patients with an increased EBV load

Patient no.	Age (yrs)	Sex[d]	Country of origin	Transplant type[a]	Time from transplantation to increased EBVL (days)[b]	EBV (copies/ml whole blood)	Immunosuppressive regimen[c]	PTLD	Status at last follow-up[e]
sLCL-2	66	m	Germany	SCT	26	3,150	CSA, MTX		Alive
sLCL-3	56	f	Germany	KT	7,456	9,870	CSA, ST	Yes[f]	Alive
sLCL-4	66	f	Spain	KT	1,821	18,600	CSA, MMF, ST		Alive
sLCL-5	64	m	Germany	SCT	29	1,000	FK, MMF		Dead (relapsed ALL)
sLCL-6	66	f	Germany	KT	3,024	1,730	ST		Alive
sLCL-7	68	m	Germany	SCT	26	2,390	CSA		Alive
sLCL-8	46	f	Russia	SCT	41	2,330	CSA		Alive
sLCL-9	64	m	Germany	SCT	35	2,600	CSA		Alive
sLCL-10	60	f	Germany	KT	2,853	1,920	BELA, ST		Alive
sLCL-11	63	m	Germany	SCT	273	16,200	FK		Alive
sLCL-12	32	m	Germany	KT	22	22,600	CSA, ST		Alive
sLCL-14	37	m	Germany	KT	810	16,400	FK, MMF, ST		Alive
sLCL-15	69	m	Germany	KT	613	1,000	BELA, MMF		Alive

[a]KT, kidney transplantation; SCT, stem cell transplantation.
[b]EBVL, EBV load.
[c]CSA, cyclosporine; MMF, mycophenolate mofetil; FK, tacrolimus; SIR, sirolimus; AZA, azathioprine; MTX, methotrexate; BELA, belatacept; ST, steroid.
[d]m, male; f, female.
[e]ALL, acute lymphoblastic leukemia.
[f]Non-EBV-associated T-cell PTLD.

partially covered with bound viruses (Fig. 1). While the EBV genome adopts a circular conformation in latently infected B cells, EBV lytic replication results in the generation of linear genomes (1). We assessed the structure of the EBV genomes present in our panel of LCLs using Gardella gel analyses. These assays revealed the presence of linear genomes in cell lines that were found to produce lytic proteins, thereby confirming that these cells supported lytic replication (Fig. 2A). We examined four cell lines that showed signs of lytic replication in electron microscopy and could confirm the presence of mature virions in the infected cell population (Fig. 2B). Interestingly, we frequently found viruses bound at the B-cell surface, confirming the results of the gp350-specific staining. This was expected, as these cells express the EBV receptor CD21. We then attempted to infect and immortalize primary B cells with supernatant from our LCL panel. Although many viruses were bound to the cell surface, this experiment nevertheless succeeded in 5/9 IM sLCLs and in 8/13 iEBVL sLCLs (Fig. 3A and B). When daughter cell lines could be established from these supernatants, they exhibited the characteristics of the cell line from which the viruses were produced in terms of gp350 and BZLF1 expression, demonstrating that the properties observed in the initial cell lines reflected the intrinsic properties of the virus (Fig. 3A and B). We then monitored the ability of the sLCLs to support lytic replication over time. Three months after establishment of the LCLs, gp350 expression decreased but remained detectable in 4 iEBVL cell lines (2 comparable to M81 and 2 weaker than M81) and in 3 IM B cell lines (3 weaker than M81) (Fig. 2C). We have previously reported a correlation between the growing characteristics of our sLCL panel and their miRNA expression profile (10). This gave us an opportunity to assess the relation between miRNA expression and lytic replication. However, we could only identify a weak correlation between miR-BHRF1-3 expression levels and the ability to support lytic replication (Pearson's *r*, 0.4836; *P* value, 0.049).

Most iEBVL and IM strains are genetically related to B95-8. We wished to identify the molecular events that govern the variable replication rates observed across the investigated panel and first turned our attention to the BZLF1 promoter. Indeed, the BZLF1 promoter contains multiple binding site for transcription factors and is considered to be a crucial regulatory element for the cell's decision to produce the BZLF1 protein (11). LCLs infected with M81 express lytic proteins at a high level, and this phenotype has indeed been ascribed to some extent to polymorphisms in the BZLF1 gene of this virus (4). Therefore, we cloned and sequenced the BZLF1 promoter, its introns, and its open reading frame from our virus panel (Table 2). We found that the sequences of all BZLF1 alleles were very close to those of Western viruses isolated from

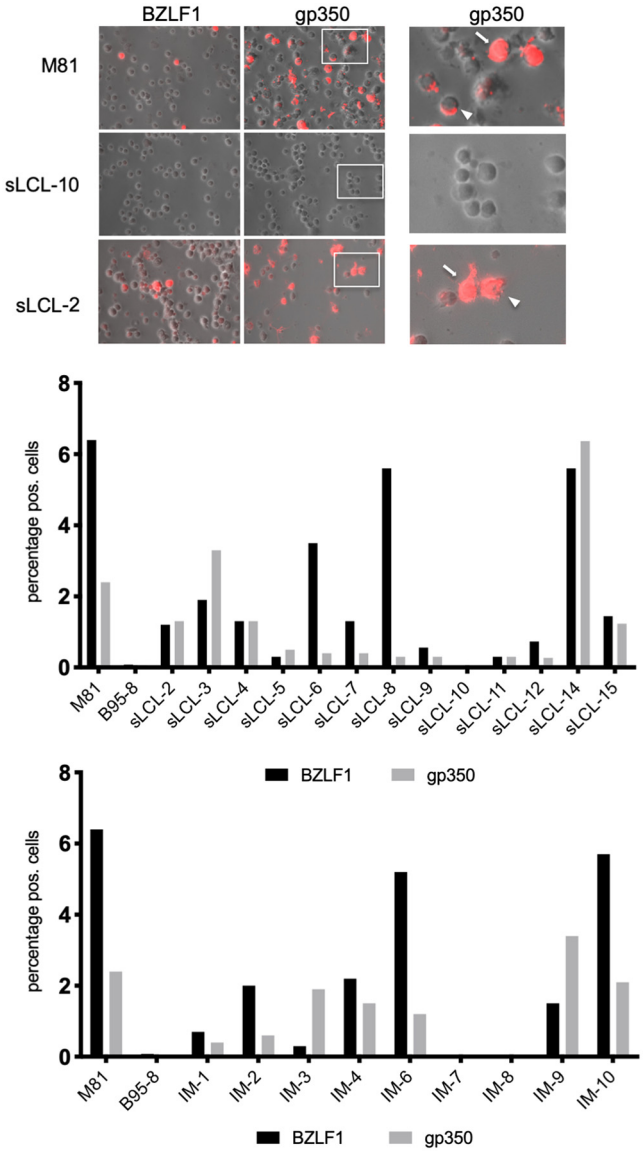

FIG 1 Multiple EBV-positive B-cell lines from Western individuals support lytic replication. Twenty-two sLCLs were immunostained with antibodies specific for BZLF1 and gp350. The pictures show the results of the staining in two of the investigated cases, together with cells infected with rM81 (white arrows, gp350-positive cells; white arrowhead, cells covered with viruses). The graphs give the percentage of BZLF1- and gp350-positive replicating cells and exclude nonreplicating cells coated with viruses.

patients with IM or PTLD, and, in particular, that they lacked the Zp-V3 polymorphism commonly found in viruses endemic in East Asia and that was recently shown to confer high replication abilities (12) (13). We noticed that viruses sharing the same BZLF1 sequence showed a highly variable propensity to replicate (compare sLCL-2 and sLCL-5 or IM-6 and IM-7; see Fig. 1), demonstrating first that the Zp-V3 polymorphism is not a prerequisite for potent and sustained spontaneous lytic replication, and second that the sequence of the BZLF1 gene is not the only parameter that governs this process. Sequencing of the EBNA2 gene showed that all viruses were of type 1 (Table 2). These data confirmed that EBV strains very close to B95-8 are dominant in Western countries.

EBV replication in LCLs is poorly sensitive to inducers. LCLs are classically refractory to lytic replication, and multiple chemical inducers have been used to increase virus production in these cells. Therefore, we investigated the sensitivity of sLCLs that had been in culture for 90 days to these molecules. We treated cells with

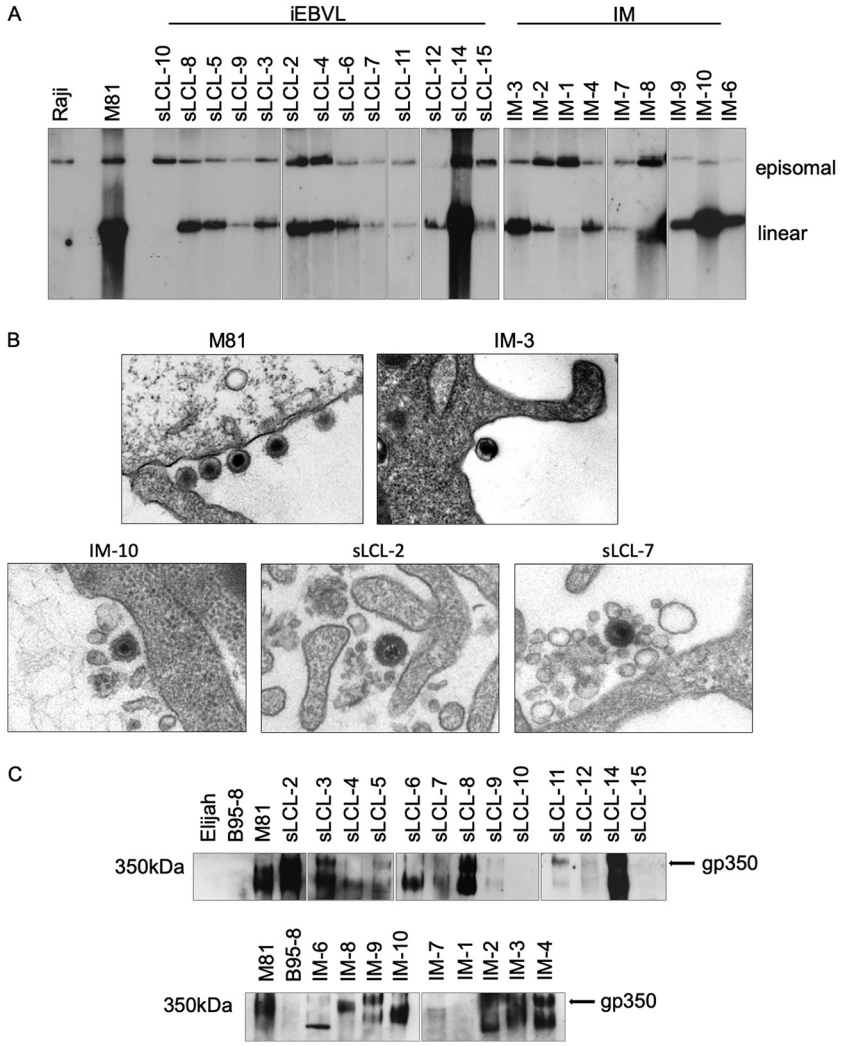

FIG 2 Multiple EBV-positive B-cell lines from Western individuals produce viruses. (A) A Gardella gel analysis was performed to identify linear viral DNA that is produced during lytic replication. M81 served as a positive control and Raji as a negative control. (B) Electron microscopy pictures showing viruses at the surface of EBV-positive B cells in five cell lines. (C) The panel of cell lines was subjected to a Western blot analysis with a gp350-specific probe. The EBV-negative Elijah cell line served as a negative control.

tetradecanoyl phorbol acetate (TPA) combined with butyrate, ionomycin, and transforming growth factor β (TGF-β). None of these substances induced lytic replication in nonpermissive sLCLs. However, when we exposed the sLCLs that supported lytic replication to TPA combined with butyrate or to TGF-β, these substances increased replication of the cell lines, on average, by 60 and 50%, respectively, although there was a large variation in the amplitude of the effect in the individual viruses (Fig. 3C). Ionomycin had, on average, hardly any effect on the replication of the sLCL panel (average 1.2 increase) (Fig. 3C). Some cell lines were more sensitive to the drug, although their absolute level of replication remained low.

Cloning of a new EBV Western strain on a BAC. To be able to accurately study the properties of a virus endowed with a high lytic replication rate, we both infected marmoset B cells with the sLCL-2 virus and cloned the viral genome onto a BAC replicon. We choose this line because it maintained high levels of gp350 over time and upon passaging to fresh B cells. The resulting marmoset cell line displayed high levels of spontaneous replication and produced infectious virus in the supernatant that is easy to harvest (Fig. 4A). To clone sLCL-2, a BACmid flanked by sequences specific to the EBV terminal repeats was introduced into marmoset B cells infected by sLCL-2 and sub-

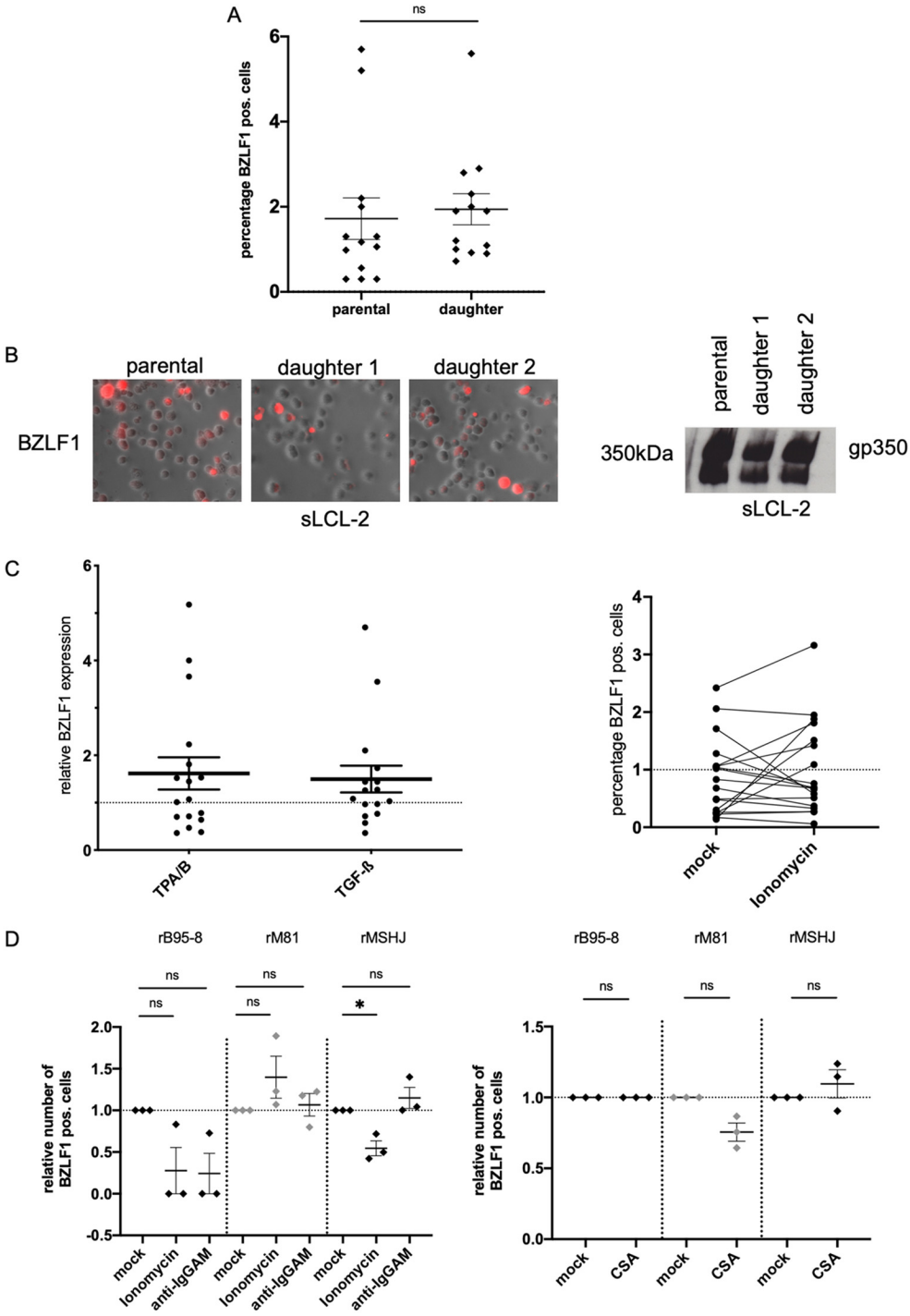

FIG 3 The ability of virus isolates to replicate is maintained in different B-cell populations and under chemical induction of lytic replication. (A) Thirteen iEBVL and IM sLCLs produced enough virus to infect another unrelated B-cell sample. The replication rate, as assessed by the percentages of BZLF1-positive B cells in the parental and daughter cell lines, is given in a dot plot. The average and standard error is also indicated. (B) We also show an example of immunofluorescence staining and a Western blot for gp350 in parental and daughter cells. (C, right). Fifteen spontaneous LCLs were treated with a combination of tetradecanoyl phorbol acetate (TPA) and butyrate, transforming growth factor β (TGF-β), or ionomycin. The left dot plot shows the fold change in the number of BZLF1-positive B cells after exposure to the first two drugs, relative to that in mock-treated cells, and the right dot plot shows the percentage of BZLF1-positive B cells in the presence of absence of ionomycin. (D) Three independent primary B-cell samples transformed with rMSHJ, rM81, and rB95-8 were treated with antibodies directed against the B-cell receptor, with ionomycin (left), or with cyclosporine (right). The dot plots show the fold change in the number of BZLF1-positive B cells relative to that in mock-treated cells.

TABLE 2 Polymorphisms in the BZLF1 gene and its promoter

Cell line[c]	Mutation(s) in BZLF1 ORF[a]	Closest EBV strain[b]
sLCL-2	C696G	E1563 Owv7 (IM)
sLCL-3		B95-8 (IM)
sLCL-4	C188G	E1583 OWv7 (IM)
sLCL-5	C696G	E1563 Owv7 (IM)
sLCL-6	G616T C696G	GC-variant-9
sLCL-7	T383C G616T	GC-variant-9
sLCL-8	G616T	GC-variant-9
sLCL-9		B95-8 (IM)
sLCL-10	G616T	GC-variant-9
sLCL-11	A411C C696G	GK_BL67
sLCL-12	A471G	E1563 Owv7 (IM)
sLCL-14	A301C	B95-8 (IM)
sLCL-15	G616T	GC-variant-9
IM-1	C163T G616T	M-ABA
IM-2		B95-8 (IM)
IM-3	C696G	E1563 Owv7 (IM)
IM-4		B95-8 (IM)
IM-6	C169T G175A C181A T213C G403A T437C T459C A471G G613T	HL04
IM-7	C169T G175A C181A T213C G403A T437C T459C A471G G613T	HL04
IM-8		B95-8 (IM)
IM-9	C169T G175A C181A T213C G403A T437C T459C A471G G613T	HL04
IM-10	G610T	GC-variant-9

[a]None of the cell lines showed mutations in the BZLF1 mini-Zp. ORF, open reading frame.
[b]IM, infectious mononucleosis; GC, gastric cancer; HL, Hodgkin lymphoma.
[c]All cell lines were EBV type A.

jected to hygromycin selection. The recombinant viral genome, dubbed rMSHJ, was rescued from hygromycin-resistant cells and introduced into *Escherichia coli* cells, in which it was subjected to restriction analysis and sequencing (Fig. 4B). This assay showed that the restriction pattern of this recombinant virus differs from the one generated by digestion of the recombinant M81 and B95-8 genomes. The rMSHJ has four terminal repeats before the BACmid and three after it. Complete sequencing of the rMSHJ genome allowed alignment to previously available viral sequences and the construction of a genetic tree (Fig. 5). In parallel, we sequenced the complete genome of the replicating IM-3 cell line to obtain a second viral sequence. Both genomes clustered with Western strains, and in particular with B95-8, although they were distinct from it (Fig. 5). We found 654 nonsynonymous mutations in rMSHJ relative to B95-8, i.e., in approximately 0.48% of the genome, and 524 in IM-3 relative to B95-8, i.e., in approximately 0.39% of the genome (Table 3). Interestingly, both viruses were closer to each other (280 mutations) than to B95-8 (Table 3). The mutations in both IM-3 and rMSHJ were homogeneously distributed across the genome (Tables 4 and 5). However, as previously noted, viral latent genes displayed on average more nonsynonymous mutations than lytic genes (14). Among latent genes, EBNA1, EBNA2, LMP1, and LMP2 were the most polymorphic (Tables 4 and 5).

Phenotypic characteristics of rMSHJ. Stable introduction of the rMSHJ genome into 293 cells allowed efficient virus production and thus detailed characterization of the virus properties. Viral titers upon induction were in the range of 5×10^7 genome equivalents per ml, as defined by quantitative PCR (qPCR), and were thus intermediate between rB95-8 (1×10^7/ml) and rM81 (1×10^7/ml). We began the characterization of rMSHJ by infecting primary B cells. Exposure of B cells to rMSHJ, rM81, and rB95-8 led to primary B-cell infection, but the infection efficiency was nearly five times higher with rB95-8 than with rMSHJ or rM81, as determined by EBNA2 (a viral protein expressed shortly after infection) staining (Fig. 6A). We then performed transformation assays in 96-well cluster plates coated with feeder cells. These assays showed that seeding of 3 EBNA2-positive B cells after infection with rMSHJ and rM81 led to a similar number of transformed colonies. However, this number was two to three times lower than that after infection with rB95-8. Thus, rB95-8 is more transforming than rMSHJ or rM81 (Fig. 6B). We complemented this approach by comparing the growth rate of LCLs freshly

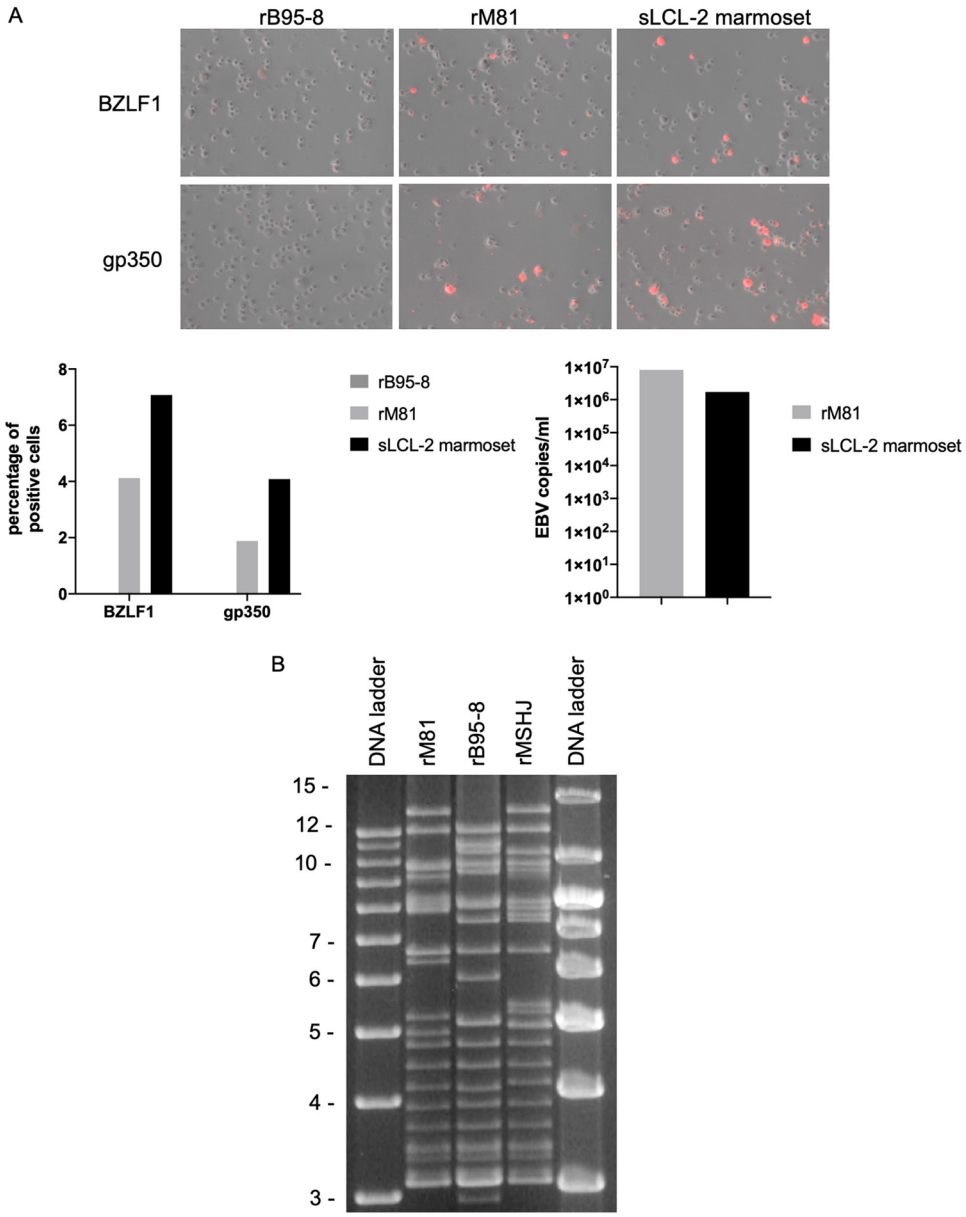

FIG 4 MSHJ replication in marmoset cell lines and its cloning as a BAC. (A) Primary B cells from the peripheral blood of marmosets were infected with sLCL-2. B cells infected by rM81 or by rB95-8 served as positive and negative controls, respectively. The picture shows BZLF1- and gp350-positive cells (red), the first graph gives the percentage of positive cells in the cell lines, and the second graph gives the viral titers in the supernatants of the cell lines, as determined by quantitative PCR (qPCR). (B) The rMSHJ, rM81, and rB95-8 genomes were digested with BamHI, and the resulting fragments separated onto an agarose gel. The size of the fragments is given by the DNA ladders.

established with the different viruses. These assays showed that B95-8-infected B cells grew more quickly than B cells after infection with rMSHJ, with B cells transformed by rM81 being the slowest (Fig. 6C). B cells transformed by these viruses showed expression of latent genes, although some variations in the expression level and size of the proteins was noted, as previously described (15) (data not shown). Some of these differences can result from the polymorphisms identified in the latent genes that lead to a variable affinity of the antibodies for the viral proteins. We then performed infections with rMSHJ, rB95-8, or rM81 on primary epithelial cells derived from the respiratory epithelium that covers the sphenoidal sinus and stained infected cells for Epstein-Barr virus-encoded RNA (EBER) expression (Fig. 7A and B) (16). We performed direct infections or transfer infections using primary B cells coated with viruses (17).

FIG 5 IM-3 and rMSHJ are closely related to B95-8. The genomes of IM-3 and MSHJ (each indicated by a dot) were aligned to 130 published EBV genomes, including that of B95-8 (indicated by a square). The genetic tree shows the degree of divergence between the sequences, and the numbers give the branch length percentage and thus the level of divergence.

TABLE 3 Nonsynonymous mutations in rMSHJ and IM-3

Comparison	No. of nonsynonymous mutations (bp)	
	IM-3	rMSHJ
To reference sequence (NC_007605.1)[a]	524	654
To the closest IM-3 neighbor (sLCL-IS1.10 Australia PTLD)[b]	93	
To the closest rMSHJ neighbor (E1563_BCv1 USA IM)[b]		122
Between IM-3 and rMSHJ[c]	280	

[a]Aligned sequence of 135,748 bp for IM-3 and 135,744 for rMSHJ (tandem repeats are not considered); GenBank accession number NC_007605.1.
[b]Aligned sequence of 135,740 bp for IM-3 and 135,741 for rMSHJ (tandem repeats are not considered).
[c]Aligned sequence of 135,745 bp (tandem repeats are not considered).

These assays showed that rMSHJ can infect epithelial cells, but with lower efficiency, 5% to 50%, relative to rM81. As previously reported, B95-8 could not infect these cells (4). We then monitored the ability of B cells infected with this virus panel to initiate and complete lytic replication. To this end, we stained B cells at weekly intervals with antibodies specific to BZLF1 and gp350 (Fig. 8A). This analysis revealed that the B-cell populations infected with rB95-8 showed some BZLF1-positive cells 1 week postinfection, although signals were weak, mainly located in the cytoplasm of infected cells and very rarely in the nucleus. These cells did not express gp350. This pattern remained visible for the following weeks, with a regular decrease in the number of BZLF1-positive cells across the 4 weeks of observation. B cells infected with rM81 and rMSHJ showed a different pattern of expression. While in both cases BZLF1 signals could be detected in the cytoplasm after 1 week of infection, cells showing BZLF1-specific nuclear signals became visible only in the third week postinfection. At this time point, a minority of infected cells were strongly gp350 positive, and the majority of cells showed viruses bound to their surface. However, the percentage of gp350-positive cells was clearly

TABLE 4 Polymorphisms of IM-3 relative to the reference genome NC_007605.1

Sequence description[a]	No. of bp considered	Polymorphism statistics				
		No. of bp	%	No. of amino acids	No. of SNPs[b]	Insertion and/or deletion (length [bp])
Region between BNLF2a ORF and LMP1 ORF	673	26	3.86		26	
oriP	1,355	30	2.21		20	Insertion (10 bp)
EBNA1 ORF	1,050	23	2.19	15	23	
BHRF1 intron	439	8	1.82		8	
Cp promoter (BCRF1 gene to W repeats)	1,719	31	1.80		29	Insertion (1 bp), deletion (1 bp)
EBNA2	1,272	20	1.57	11	17	Insertion (3 bp)
LMP2A exon 1	448	7	1.56	5	7	
BRRF2 ORF	1,614	23	1.43	12	23	
LMP1 ORF	842	11	1.31	9	11	
RPSM1 promoter part between BART.I and BART.Ia	966	11	1.14		9	Insertion (1 bp), deletion (1 bp)
BDLF3 ORF	705	7	0.99	3	7	
BBLF4 ORF	2,430	20	0.82	5	20	
EBNA3C ORF + intron	2,746	22	0.80	11	22	
BBLF2/BBLF3 ORF	2,130	14	0.66	4	11	
BDLF2 ORF	1,263	8	0.63	4	8	
BNRF1 ORF	3,957	25	0.63	9	25	
BGLF3 ORF	999	6	0.60	1	6	
BRLF1 ORF	1,818	10	0.55	4	10	
Partial LMP2B gene (genome nt 1–1691)	1,691	9	0.53	1	9	
BGLF1 ORF	1,521	7	0.46	2	4	Deletion (3 bp)
BPLF1 ORF	8,700	37	0.43	15	37	
EBNA3A ORF	2,835	11	0.39	7	11	
BBRF1 ORF	1,842	7	0.38	1	7	
BOLF1 ORF	3,720	12	0.32	4	9	Insertion (3 bp)
BSLF1 ORF	2,625	4	0.15	1	6	
Total (% of total)	49,360 (36.4)	389 (74.2)		124	365 (69.7)	

[a]Sequences that had the largest numbers of polymorphisms. nt, nucleotide; ORF, open reading frame.
[b]SNP, single-nucleotide polymorphism.

TABLE 5 Polymorphisms of rMSHJ relative to the reference genome NC_007605.1

Sequence description[a]	No. of bp considered	Polymorphism statistics				
		No. of bp	%	No. of amino acids	No. of SNPs[b]	Insertion and/or deletion (length [bp])
EBER2 promoter before EBER2	74	4	5.41		4	
Region between BNLF2a ORF and LMP1 ORF	673	19	2.82		19	
Region between BMRF2 ORF and BSLF1 gene	537	15	2.79		14	Insertion (1 bp)
BDLF3 ORF	705	17	2.41	6	17	
oriP	1,355	29	2.14		19	Insertion (10 bp)
EBNA1 ORF	1,050	22	2.10	15	22	
BHRF1 intron	439	8	1.82		8	
Cp promoter (BCRF1 gene to W repeats)	1,719	30	1.75		28	Insertion (1 bp), deletion (1 bp)
LMP2A exon 1	448	7	1.56	6	7	
BRRF2 ORF	1,614	24	1.49	12	24	
LMP1 ORF	842	11	1.31	9	11	
EBNA2	1,272	15	1.18	8	15	
RPSM1 promoter part between BART.1 and BART.la	966	11	1.14		8	Insertion (1 bp), deletion (2 bp)
BGLF1 ORF	1,521	17	1.12	2	14	Deletion (3 bp)
BDLF4 ORF	678	7	1.03	2	7	
BBLF4 ORF	2,430	20	0.82	5	20	
BGLF3 ORF	999	8	0.80	1	8	
EBNA3C ORF + intron	2,746	21	0.76	10	21	
BDLF1 ORF	906	6	0.66	1	6	
BBLF2/BBLF3 ORF	2,130	14	0.66	4	14	
BDLF2 ORF	1,263	8	0.63	4	8	
BNRF1 ORF	3,957	25	0.63	9	25	
Partial LMP2B gene (genome nt 1–1691)	1,691	10	0.59	1	10	
BXRF1 gene	2,578	15	0.58	1	15	
BRLF1 ORF	1,818	10	0.55	4	10	
BALF4 ORF	2,574	12	0.47	4	12	
BcLF1 ORF	4,146	19	0.46	2	19	
BPLF1 ORF	8,652	37	0.43	15	37	
EBNA3A ORF	2,835	11	0.39	7	11	
BBRF1 ORF	1,842	7	0.38	1	7	
BOLF1 ORF	3,723	12	0.32	4	9	Insertion (3 bp)
BSLF1 ORF	2,625	6	0.23	2	6	
Total (% of total)	61,263 (45.2)	477 (72.9)		135	464 (69.6)	

[a]Sequences that had the largest numbers of polymorphisms. nt, nucleotide; ORF, open reading frame.
[b]SNP, single-nucleotide polymorphism.

higher in cells infected with rM81 than that in those infected with rMSHJ. This pattern remained similar for another 3 weeks, with a steady increase in the number of replicating cells. At 6 weeks postinfection, the number of B cells infected with rM81 that produced BZLF1 was on average higher than that of their counterparts infected with rMSHJ, and the difference was even more pronounced for gp350 (Fig. 8B). A Western blot analysis confirmed expression of these lytic proteins after infection with rM81 and rMSHJ1, although infection with the former led to stronger gp350 expression (Fig. 8C). This assay also showed that the BZLF1 protein produced by cells infected with rMSHJ has a lower molecular weight than that of the species produced by cells infected with rM81. This difference was previously noted after transfection of the B95-8 BZLF1 gene (4).

B cells infected with rMSHJ replicate in an *in vivo* murine model. We wished to confirm some of our data in an *in vivo* animal model. Therefore, we injected primary B cells coated with rMSHJ or rM81 into immunosuppressed NSG-A2 mice (18). Five weeks after injection, mice developed tumors. Immunohistological stains revealed that for both viruses, these tumors expressed both BZLF1 and gp350 (Fig. 8D). We found that 8.7% of EBER-positive cells underwent replication 5 weeks postinfection as assessed by BZLF1 expression after infection with rMSHJ, compared with 7.2% after infection with rM81. Thus, there is a good correlation between the *in vitro* and the *in vivo* data, although tumors *in vivo* could only be analyzed at a single time point (5 weeks postinfection). Injection of the IM-3 cell line revealed a similar pattern, although gp350 was less strongly expressed (data not shown).

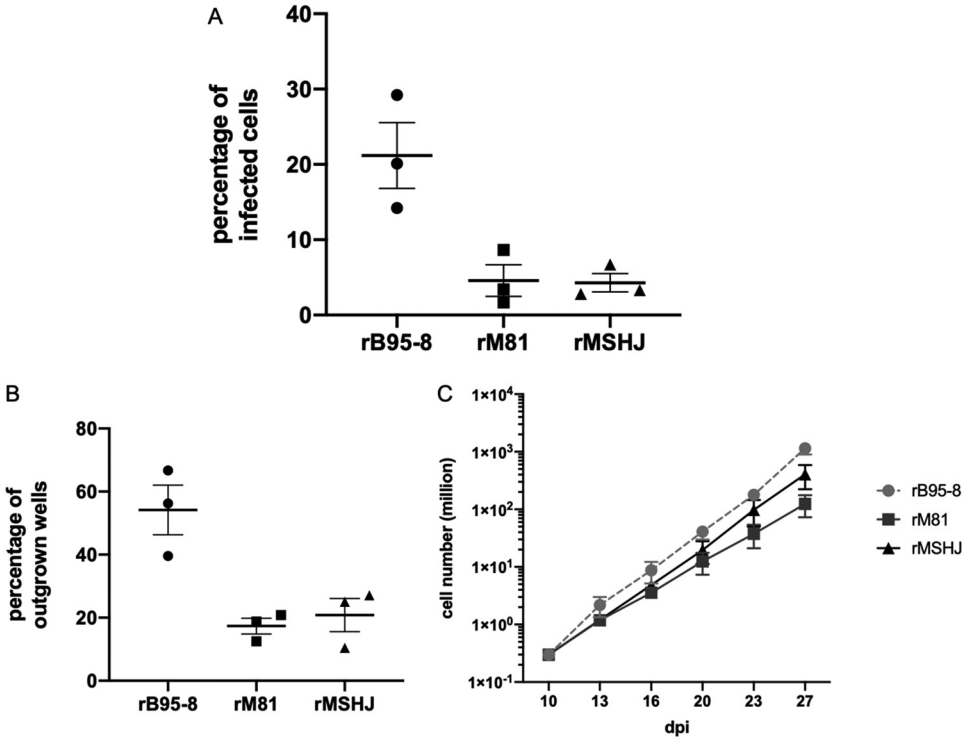

FIG 6 rMSHJ B-cell tropism and transformation efficiency. (A) Three independent sets of primary B cells were infected with rMSHJ, rM81, and rB95-8 at the same multiplicity of infection (10 genome equivalents per cell). Three days later, cells were stained for the EBNA2 protein. The dot plot shows the percentage of infected B cells. (B) Three independent sets of primary B cells were infected with rMSHJ, rM81, and rB95-8 at the same multiplicity of infection (10 genome equivalents per cell). Three days after infection, cells were stained for EBNA2. Infected cells were seeded in a 96-well cluster plate at a concentration of three EBNA2-positive cells per well. Five weeks later, the percentage of outgrown wells was determined. The results are given in the dot plots. (C) Cells from LCLs generated with rMSHJ, rM81 and rB95-8 (3×10^5) were kept in culture for 4 weeks to generate the growth curves reproduced in the graph.

B cells infected by rM81 or rMSHJ are responsive to a Btk-specific inhibitor. The role of the B-cell receptor (BCR) signaling complex on EBV lytic replication has been well established, and we wished to study its impact on spontaneously replicating EBV-infected B cells. To this end, we transformed a set of three independent B-cell samples with rB95-8, rM81, or rMSHJ and exposed them to ionomycin or to immunoglobulins directed against the B-cell receptor to activate calcium-dependent pathways. While the latter treatment had no statistically significant effect on the replication rate of any of the different types of infected cells, the former potentiated it only in one cell sample infected by rM81 (Fig. 3D). We then blocked calcium signaling in these cells by exposing them to cyclosporine. This treatment led to an average 30% reduction in the number of BZLF1-positive B cells infected by rM81 that did not reach statistical significance, but had no effect in B cells infected with rB95-8 or rMSHJ (Fig. 3D). We extended our investigations to modulators of the proximal arm of the BCR cascade by treating our panel of cell lines with ibrutinib at concentrations known to inhibit Btk only (10 nM) (19). This led to a clear reduction of lytic replication in B cells infected with rM81 and with rMSHJ, although the effects were less pronounced in the latter case (Fig. 9A). As expected, the treatment with ibrutinib led to a reduction in the amounts of p-Btk and p-Akt-1, two of its downstream targets, in treated LCLs (Fig. 9B). All tested LCLs expressed p-Btk irrespective of their ability to support lytic replication (Fig. 9B). Increase of ibrutinib to 100 nM completely inhibited replication. Importantly, exposure to ibrutinib at both concentrations did not affect cell viability or cell growth (Fig. 9C and D). Similar, although less pronounced, effects were observed in B cells infected by rMSHJ. Finally, we exposed infected cells to the mTORC1 inhibitor rapamycin, which was

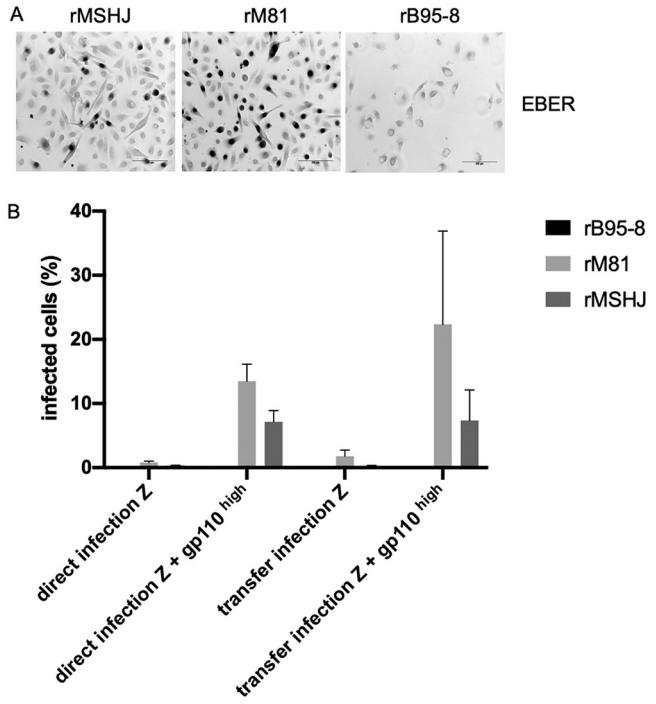

FIG 7 rMSHJ epitheliotropism. Primary epithelial cells were infected with rMSHJ, rM81, and rB95-8 at the same multiplicity of infection (100 genome equivalents per cell), using either direct or transfer infection on primary B cells. Three days later, cells were subjected to *in situ* hybridization with a probe specific for the highly abundant noncoding RNA EBER. (A) Representative example of transfer infection. (B) The bar graph shows the percentage of infected cells under the different conditions studied after infection of 3 samples. Cells were infected with viruses that express gp110 at high or low levels. We give the mean and standard error from three infection experiments.

previously reported to inhibit induced lytic replication (20, 21). This treatment indeed nearly completely blocked BZLF1 expression in both B cells transformed by rMSHJ and B cells transformed by rM81, but it substantially decreased cell viability and division (Fig. 9A, C and D).

Infected B cells that have lost permissivity to spontaneous EBV replication can be rescued by hypoxia treatment. Previous reports have shown that iron chelators that mimic hypoxia potentiate lytic replication in infected BL cells (22). We wished to test whether hypoxia also modulated spontaneous lytic replication in infected B cells. To this end, we grew B cells that had been infected with rB95-8, rM81, and rMSHJ for 30 days in a hypoxic chamber (1% oxygen) for up to 1 week and monitored BZLF1 protein expression in these cells. This treatment had no effect on B cells infected with rM81 or rMSHJ (Fig. 10A). However, we observed the appearance of nuclear BZLF1 signals in cells infected with rB95-8, although the percentage of positive B cells remained between 0.07 and 0.6%. We repeated this experiment with LCLs that had been in culture for more than 3 months and whose replication rates were reduced by 80% relative to that at their peak. Hypoxia led to a 3- to 4-fold increase in the number of BZLF1-positive B cells infected by rMSHJ or rM81 and again to the appearance of a few B95-8-transformed B cells with genuine BZLF1-positive nuclear signals ($<$0.5%) (Fig. 10A). Western blotting also showed upregulation of BZLF1 and gp350 after infection with rM81 and rMSHJ (Fig. 10A). We also observed a parallel decrease in LMP1 expression as the result of hypoxia treatment, associated with a reduction in the molecular weight of EBNA2. These changes correlated with an increase in apoptosis, as assessed by the appearance of cleaved PARP. We then investigated tumors induced by rM81 and rMSHJ infection in immunosuppressed mice to study the relationship between vascularization and lytic replication. Previous work had found that replicating cells were located at distance from vessels, suggesting that replication was facilitated

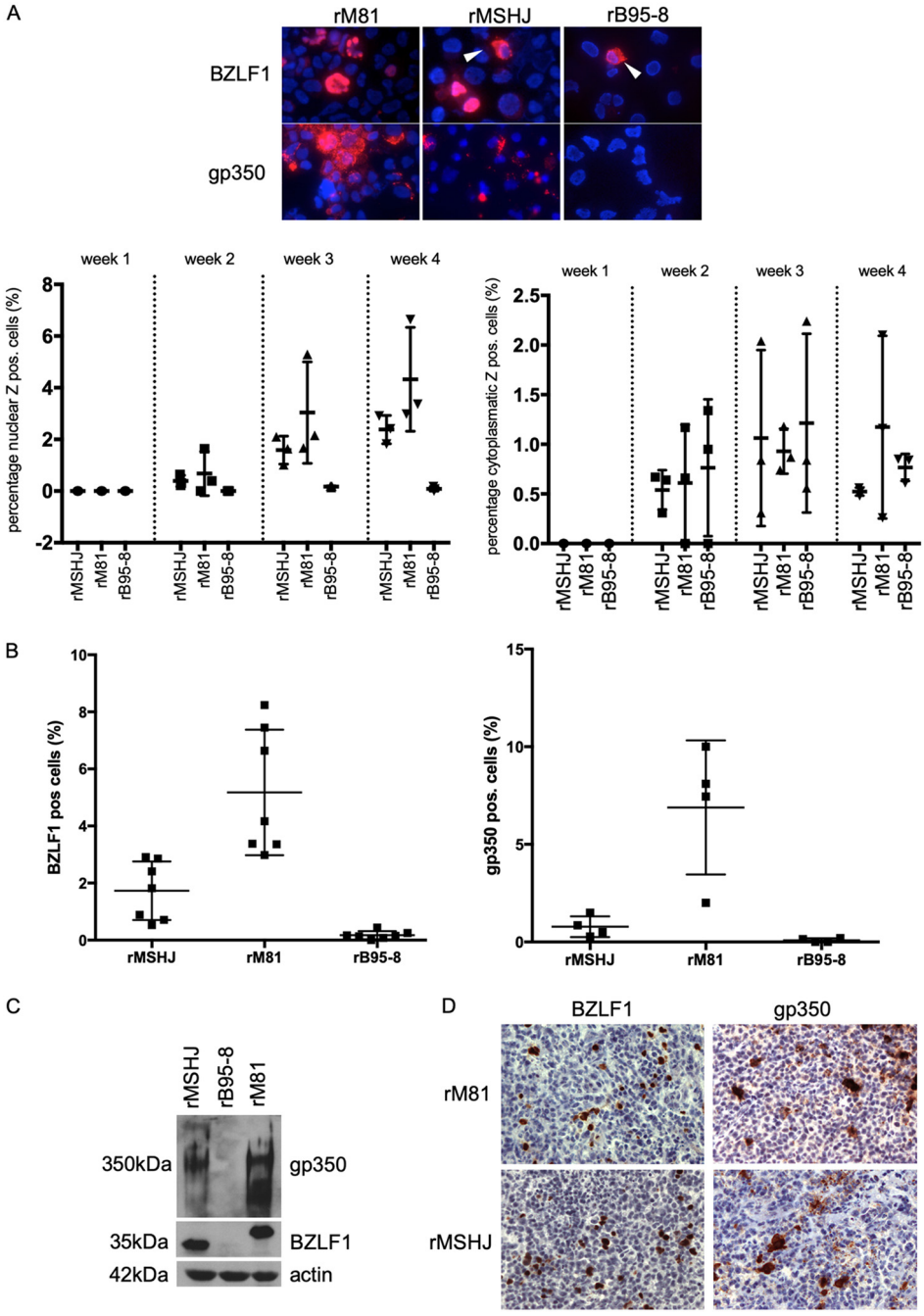

FIG 8 B cells infected with rMSHJ undergo a high level of spontaneous lytic replication. Three sets of independent primary B-cell samples were infected with rMSHJ, rM81, and rB95-8. Expression of BZLF1 and gp350 was monitored once a week for 4 weeks. (A) Example of immunostaining with BZLF1 and gp350. BZLF1 signals were detected in the nucleus, but also in the cytoplasm (white arrowheads), of infected cells. The dot plots show the percentage of cells displaying nuclear (left) or cytoplasmic (right) over time. (B) Six weeks after infection, infected cells were subjected to immunofluorescence staining with antibodies specific for BZLF1 and gp350. The percentage of positive cells is given in the dot plots together with the standard error. (C) BZLF1 and gp350 expression in one B-cell sample infected with the three viruses, as determined by Western blot. Staining for actin expression was used as a loading control. (D) The pictures show expression of BZLF1 and gp350 in EBV-positive lymphoid tumors that developed in immunosuppressed mice after infection with rM81 or rMSHJ.

by a more hypoxic environment (22). This approach used an experimental system that visualizes larger vessels but not microvessels or capillaries. However, tissue oxygenation mainly depends on microvessels that are too small to be visible with this method (23). Therefore, we stained tissues for both BZLF1 and CD34, a marker of endothelial cells

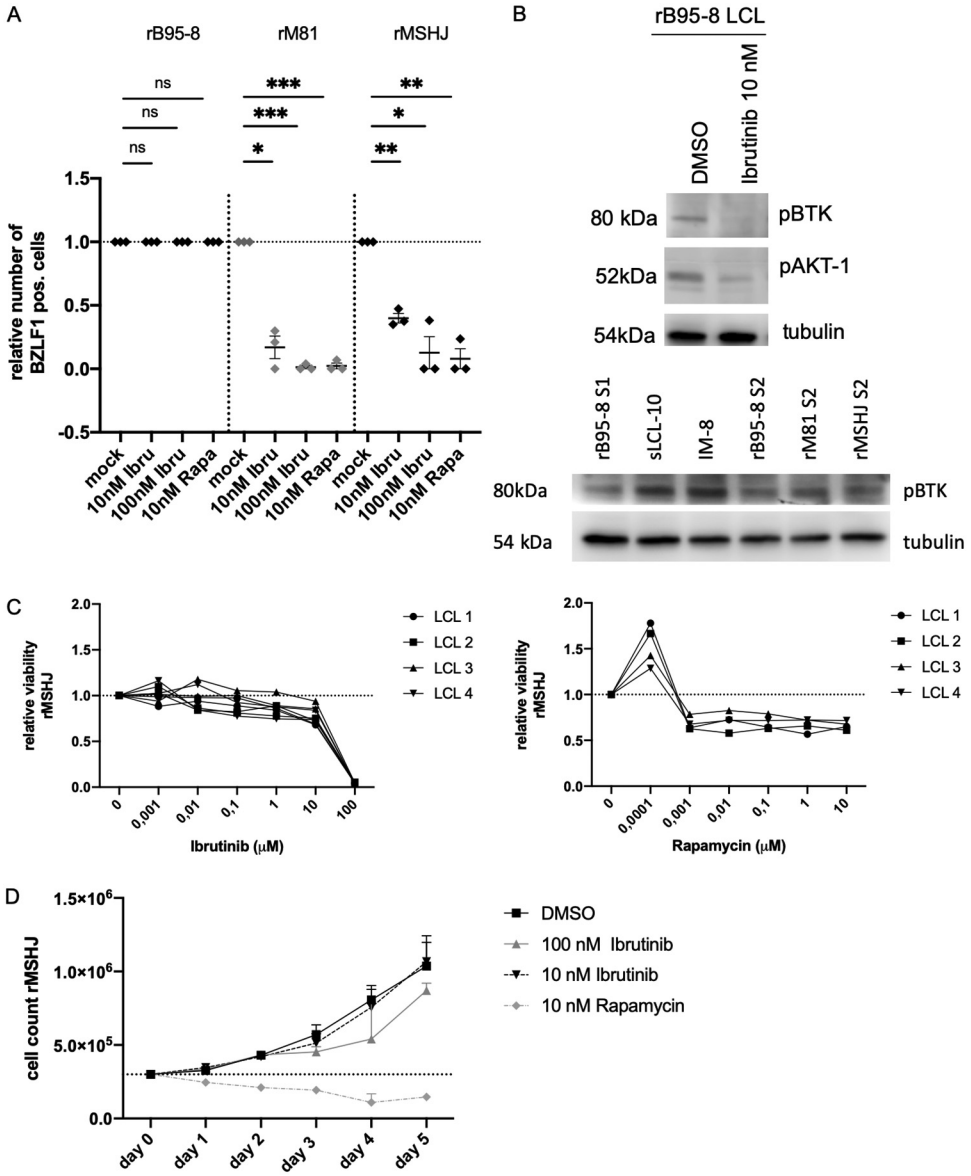

FIG 9 B cells infected with rMSHJ are sensitive to ibrutinib and rapamycin treatment. (A) Three independent primary B-cell samples transformed with rMSHJ, rM81, and rB95-8 were exposed to ibrutinib (10 nM or 100 nM) or rapamycin (10 nM). (B) Western blot showing expression p-Btk and pAKT-1 in rB95.8-transformed B cells with or without 10 nM ibrutinib treatment (upper). Western blot showing p-Btk expression in B cells transformed by viral strains S1 and S2 in blood samples 1 and 2 (lower). (C) Viability of 4 EBV-transformed B-cell samples (LCL 1 to LCL 4) after treatment with increasing concentrations of ibrutinib or rapamycin. (D) Cell growth rate of an EBV-transformed B-cell sample after treatment with different concentrations of ibrutinib or rapamycin.

(24). This approach showed that all BZLF1-positive B cells are located in the direct vicinity of capillaries (Fig. 10B), although the distance of these cells to large arteries varied more widely, ranging from 20 to 650 μm, with a mean distance of 400 μm (Fig. 10C). Therefore, we can confirm that replicating B cells are enriched at a certain distance from larger blood vessels, but this does not translate into a significant distance from capillaries.

DISCUSSION

EBV infects primary B cells and epithelial cells, but the outcome of infection is classically different in these two types of cells. While infected B cells initiate unlimited cell growth, epithelial cells support lytic replication (1). This dichotomy is based on early

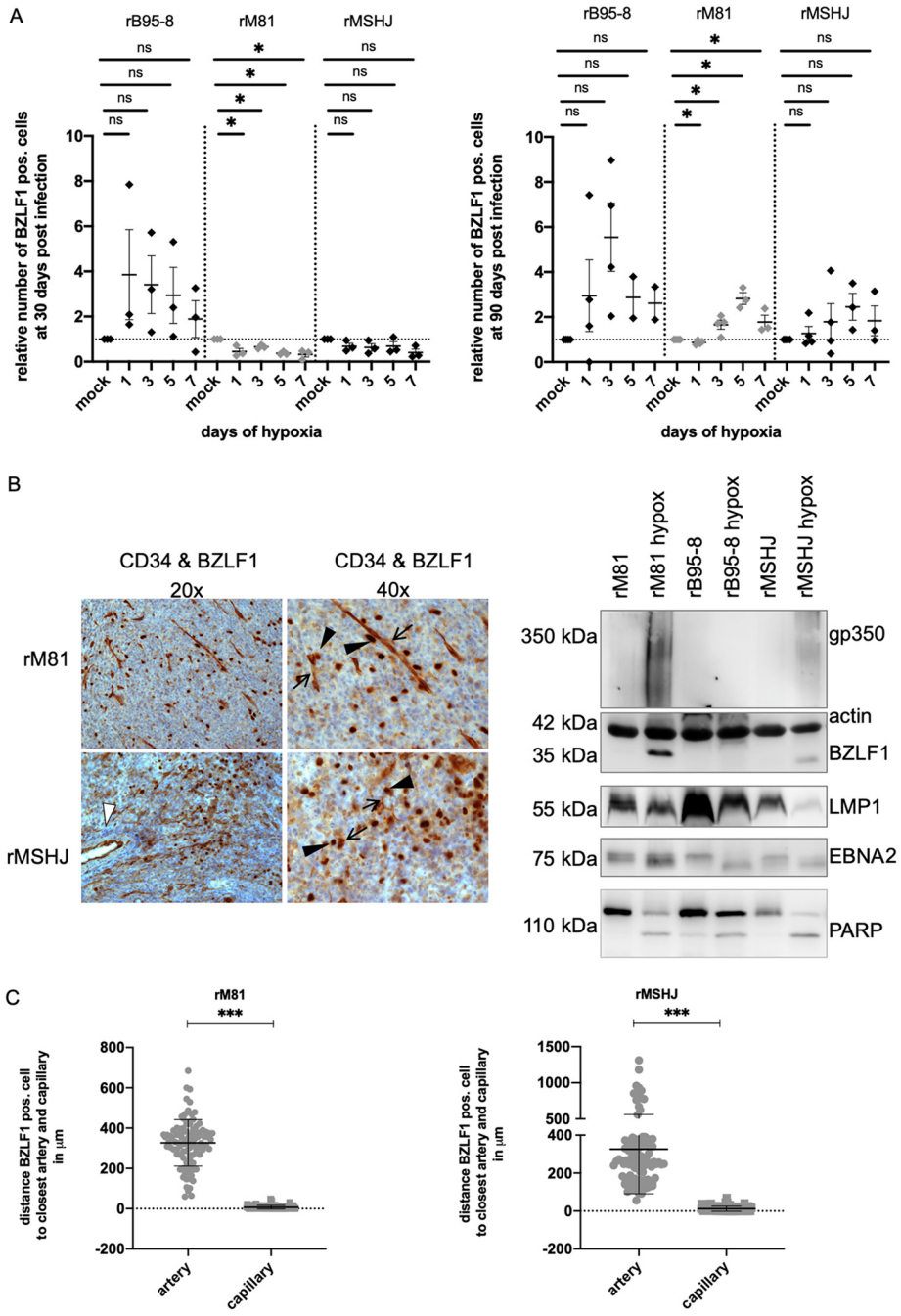

FIG 10 Hypoxia reactivates lytic replication, and lytically replicating cells are located closed to capillaries. (A) Three independent primary B-cell samples, each transformed with rMSHJ, rM81, and rB95-8 were kept under hypoxia for up to 7 days. The percentage of BZLF1-positive cells was determined after 1, 3, 5, and 7 days of hypoxia. The experiment was performed with 30- (left) or 90-day-old (right) transformed B-cell samples. One 90-day-old cell sample set was analyzed after hypoxia treatment by Western blotting using antibodies specific to BZLF1, gp350, LMP1, EBNA2, actin, and PARP. (B) Immunohistochemistry showing CD34-positive small arteries (white arrowhead) and capillaries (arrow), together with BZLF1-positive B cells (arrowhead). We show one sample infected with rM81 and one sample infected with rMSHJ at low (×20) and high (×40) power. (C) We measured the shortest distance between 100 BZLF1-positive B cells and the closest capillary or small artery. The results are given as dot plots for tissues infected with rM81 (left) and rMSHJ (right).

investigations that showed that infection of primary B cells with the prototypical B95-8 strain does not lead to any measurable virus production, although the cellular background also modulates this property (25, 26). Similarly, early reports showed that spontaneously growing LCLs from individuals with IM did not produce any virus (27).

However, approximately half of solid organ or bone marrow transplant recipients carry B cells that showed some signs of lytic replication, for example, the presence of BZLF1 or gp350 transcripts or of linear DNA, suggesting that they are infected by particular strains or that the clinical context markedly modifies the balance between the virus and its host (28–32). Similarly, spontaneously growing LCLs from healthy individuals or from patients with rheumatoid arthritis displayed variable level of viral capsid antigen (VCA) production that, however, never exceeded 1% of the infected cells (27). Interestingly, B cells infected by type 2 viruses produced viral capsid antigen in Western blot analysis at much higher levels than those infected with their type 1 counterparts (33). We now show that most samples of a panel of Western type 1 viruses showed evidence of some degree of lytic replication, coupled in many cases to spontaneous virus production, that was visible in electron microscopy and allowed passaging of the virus to uninfected B cells, a property that was not investigated in most previous studies. These daughter cell lines retained the ability to produce viruses, suggesting that this property is largely virus specific. Some transformed B-cell samples were exclusively latently infected and could not been induced to produce virus after treatment with TPA and butyrate. Because these viruses cannot be passaged to other B cells, we cannot formally exclude the possibility that they might have replicated in B cells from other individuals. Altogether, these data confirm earlier studies that many type 1 EBV-transformed B cells express low levels of lytic proteins for a limited period of time, with an essentially abortive profile characterized by a gp350 expression in up to 1% of the cells. However, they also show that 3 out of 22 of Western type 1 viruses induce an unusually potent and sustained lytic replication in infected B cells. The identification of potent lytic replication in B cells from transplant recipients or IM patients suggests that these cells are at an increased risk of genetic instability (9). In this line, it is important to note that a large subset of PTLD carry indeterminate genetic abnormalities (34).

A strict comparison between our strongly replicating EBV isolates and M81 isolates is not meaningful, as they infected different cells, had been growing for a variable length of time and also because the antibodies used in immunostains recognize lytic proteins with variable affinity owing to polymorphisms. However, infection of the same B cells with rM81 and rMSHJ showed that the rM81 replication rate remains clearly higher *in vitro*. Inducers of lytic replication such as TPA, ionomycin, TGF-β, or modulators of the B-cell receptor generally only weakly enhanced the replication rate. This suggests that the pathways successfully activated by these drugs in other EBV replication cellular systems have comparatively little influence on infected primary B cells permissive to spontaneous replication.

Cloning and study of rMSHJ revealed differences between EBV strains. In contrast to rB95-8, which induces a transitory lytic protein expression within 1 week of infection, rM81 and rMSHJ infection led to sustained lytic protein expression that began only at 3 weeks postinfection, as previously described for rM81 (4). This suggests that multiple events must take place in the infected cell before replication can start, one of which is presumably DNA methylation of the viral genome. Indeed, BZLF1 preferentially binds to methylated DNA (35). A second difference was that while replicating cells infected by rM81 and rMSHJ mainly showed nuclear BZLF1 expression with a few cells showing cytoplasmic signals, cells infected by rB95-8 mainly displayed BZLF1-specific cytoplasmic signals. This suggests the existence of a mechanism that regulates the location of the protein within different cell compartments. Finally, B cells infected by rMSHJ and rM81, but not those infected by rB95-8, produced late proteins such as gp350 but also infectious virus, suggesting that polymorphisms in the B95-8 genome cells reduce both initiation and completion of the lytic cycle.

Sequencing of rMSHJ and IM-3 confirmed their close proximity with B95-8, although they differed by 654 and 524 nucleotides, respectively. The polymorphisms were distributed across the genome, and it remains unclear at this stage which of these explain the varied ability of these viruses to replicate. Sequencing of the BZLF1 open reading frame and mini-Zp promoter thereof in our complete virus panel revealed that all of them are within the Western group, and 21/22 viruses are within the B95-8 subgroup

and lack the Zp-V3 polymorphism. This fits with previous reports showing that patients with IM carry viruses that are very closely related to B95-8 (36). However, the replicating abilities of these strains varied widely, suggesting that polymorphisms outside BZLF1 modulate this property. Other genetic elements, such as EBER2, have been found to modulate the ability of some viral strains to support spontaneous lytic replication (37). We conclude that although some Western viruses are genetically close to B95-8, they are sufficiently polymorphic to display variable properties. Which viral genes govern spontaneous lytic replication in B cells infected with rMSHJ will be revealed by the analysis of the polymorphisms between rM81, rMSHJ, and rB95-8. RM81-infected B cells showed an inconstant and weak sensitivity to modulation of the B-cell receptor pathway through treatment with cyclosporine or ionomycin. B cells infected by rMSHJ or rB95-8 were even less sensitive to these treatments.

In contrast, Btk was required for a potent spontaneous lytic replication both after infection with rMSHJ and rM81 (Fig. 9A). This inhibitor reduced the levels of p-Btk and downstream pAkt-1 in treated cells (Fig. 9B). This treatment did not affect cell viability or cell growth (Fig. 9C and D). Treatment of induced BL cells with ibrutinib was previously reported to prevent lytic replication, although the doses used in this study were much higher and probably inhibited other kinases and cell viability (Fig. 9C and D) (20). As ibrutinib has been extensively used in the treatment of lymphomas at doses similar to those used in this study, this drug might show therapeutic properties in EBV-associated diseases in which lytic replication is high, such as chronic EBV infection or even some cases of PTLD. Rapamycin has similar properties, suggesting that mTORC1 is important for all types of EBV lytic replication, although it is unclear which of the multiple targets of this kinase are important for this process (20, 21). We confirmed that hypoxia activates spontaneous lytic replication of both rM81 and rMSHJ, but only in cells that had lost permissivity after several months in culture. In contrast, hypoxia had no effect on spontaneous lytic replication at its peak, 1 month postinfection. Similarly, analysis of tissues infected by rMSHJ and rM81 showed efficient replication in cells located very close to capillaries, confirming that hypoxia is not strictly necessary for spontaneous replication.

In conclusion, we identified strongly replicating type 1 Western viruses that are closely related to B95-8, do not display the Zp-V3 polymorphism and are sensitive to ibrutinib. In contrast to rB95-8, rMSHJ will allow the genetic analysis of all EBV viral functions.

MATERIALS AND METHODS

Spontaneous cell lines. Thirteen spontaneously growing LCLs were established from B cells of 13 immunosuppressed patients with increased EBV load (iEBVL) (sLCL-2 to sLCL-15, excluding sLCL-13), and nine sLCLs were generated form the B cells of nine immunocompetent patients suffering from IM (IM-1 to IM-10, excluding IM-5). An iEBVL was defined by >1,000 copies/ml, as determined by qPCR of a whole-blood sample. The ethics committee of the University of Heidelberg approved the study (approval S/005-2014). Patients suffering from IM were diagnosed in Munich, Germany, by the detection of EBV-specific IgM antibodies and were recruited to the IMMUC study (approval 112/14). B cells (1×10^5) from the blood of patients with IM or iEBVL were purified and seeded onto NHDF feeder cells. These peripheral-blood CD19-positive ($CD19^+$) B cells were isolated by Ficoll density gradient followed by selection with anti-CD19 PanB Dynabeads and detachment of the beads (Invitrogen). Control cell lines included LCLs generated with rM81 and rB95-8, as well as the Burkitt's cell lines Raji and Elijah (EBV-negative clone thereof). The M81 virus was isolated from a Hong Kong NPC cell line (38). B95-8 was isolated from a U.S. patient with infectious mononucleosis (39). Raji is an EBV-positive BL cell line (40). The rMSHJ cell line was generated by infection of common marmoset peripheral B cells with EBV sLCL-2 virus that was isolated from a German stem cell transplant recipient with iEBVL (Table 1).

BAC cloning. A pMBO131-based plasmid carrying a prokaryotic F-factor origin of replication, the chloramphenicol (Cam) resistance marker for prokaryotic selection, an SV40 promoter-driven hygromycin gene for eukaryotic selection, and a cytomegalovirus promoter-driven enhanced green fluorescence gene was used as a basis for the targeting vector (B951) (4). B951 was flanked with two half-terminal repeats to generate the targeting vector. Ten million marmoset B cells transformed by the virus that infects sLCL-2 were electroporated with 10 μg of the targeting vector (270 V, 960 μF) and incubated in 10 ml RPMI-20% FBS for 16 h at 37°C. A total of 10^4 cells per well were plated onto 96-well U-bottomed plates in RPMI-10% FBS + 75 μg/ml hygromycin. Four weeks later, circular DNA from 15 hygromycin-resistant clones was prepared and transformed into *E. coli* strain DH10B (41). DNA from Cam-resistant colonies (15 μg/ml) was prepared and cleaved with the BamHI restriction enzyme. BAC DNA from one of

TABLE 6 Antibodies used

Antibody	Clone[a]	Dilution	Provider
gp350	72A1 (mouse, IF)	1:30	R. Feederle
gp350	OT6 (mouse, IHC)	1:600	J. M. Middeldorp
BZLF1	BZ.1 (mouse)	1:200	R. Feederle
Actin	ACTN05 (mouse)	1:10,000	Dianova
LMP1	S12 (mouse)	1:4,000	BD Pharmingen
EBNA2	PE2(mouse)	1:100	R. Feederle
EBNA1	IH4 (rat)	1:100	R. Feederle
LMP2A	15F9 (rat)	1:50	R. Feederle
EBNA3C	6C9 (rat)	1:100	R. Feederle
EBNA3B	A10-E3C (mouse)	1:100	R. Feederle
EBNA3A	E3AN-4A5 (rat)	1:100	R. Feederle
PARP	9542 (rabbit)	1:1,000	Cell Signaling
CD34	EP373Y (rabbit)	1:200	Abcam

[a]IF, immunofluorescence; IHC, immunohistochemistry.

these clones (B048, dubbed rMSHJ) contained a complete genome whose restriction pattern was partly similar to the one observed in the recombinant B95-8 and M81 strains. This DNA was amplified and transfected into HEK293 cells (1 μg DNA per 4 $\times$ 10^5 cells) using lipofection (Metafectene; Biontex). Cells were seeded onto 150-mm culture plates in RPMI supplemented with 10% FBS and hygromycin (100 μg/ml). Multiple green fluorescent protein (GFP)-positive colonies were expanded 4 weeks post-transfection and tested for their ability to produce virus particles upon induction of the lytic cycle. The recombinant B95-8 and M81 BAC clones were previously described (4).

Sequencing and alignment. The B048 clone was sequenced by high-throughput sequencing with an Illumina HiSeq 2000 platform and assembled using GS Reference Mapper software. This analysis showed that the recombination occurred between the terminal repeat (TR) in MSHJ and M81, between nucleotides 101 and 344 from the MSHJ TR and between nucleotides 83 and 326 from the M81 TR. The sequences of the ambiguous regions and the repeat regions were further confirmed using a standard Sanger sequencing method.

To perform alignments, the currently available EBV genome sequences were downloaded from the NCBI database. The EBV genomes were aligned with Multiple Alignment using Fast Fourier Transform (MAFFT) v7.419 software (42). The phylogenic tree was generated with MEGA7 software using the minimum-evolution method.

Gardella gel electrophoresis and Southern blot analysis. Cell lines were analyzed for evidence of linear or episomal viral DNA using the agarose gel electrophoresis method described by Gardella et al. (43). In this method, 5 $\times$ 10^5 infected B cells were lysed in gel slots to avoid shearing of the viral DNA they carry. Southern blot hybridization was performed as described before using a P32-labeled probe directed against nonrepetitive sequences specific to the EBV gp350 gene locus (44).

Immunostaining and Western blot analysis. Cells were fixed with 4% paraformaldehyde (BZLF1 and EBNA2) or acetone (gp350) for 20 min at room temperature. Paraformaldehyde (PFA)-fixed cells were permeabilized in phosphate-buffered saline (PBS) 0.5% Triton X-100 for 2 min. Fixed cells were incubated with the first antibody at 37°C for 30 min, washed in PBS thrice, and incubated at 37°C for 30 min with the secondary antibody conjugated to cyanine 3 (Cy3). Slides were embedded with 90% glycerol and visualized with a Leica DM5000 B epifluorescence microscope. Western blotting for viral proteins was performed as described before (45). For detection of EBNA1, EBNA2, EBNA3A/B/C, BZLF1, PARP, and LMP-1, 50 μg of total proteins was denatured with beta-mercaptoethanol and loaded onto a 10 or 12.5% SDS acrylamide gel. For detection of gp350, 50 μg of nondenatured proteins were loaded onto a 7.5% SDS acrylamide gel. The list of antibodies used in this study is given in Table 6.

Electron microscopy. A sample of 6 $\times$ 10^6 cells was centrifuged for 10 min at 400 rpm. Further preparation, embedding, and sectioning were carried out as described previously (46). Ultrathin sections were examined by electron microscopy (EM900; Zeiss).

Virus production. For recombinant virus production, lytic replication of 293/rMSHJ, 293/rM81, and 293/rB95-8 was induced by transfection of a BZLF1 expression plasmid with or without cotransfection of a BALF4 expression plasmid, as described previously (45). The supernatants were collected 4 days posttransfection and filtered through a 0.45-μm filter to remove cell debris.

qPCR. We performed qPCR to determine the EBV viral load in supernatants from producer cell lines. Briefly, 44 μl of the tested samples was treated with 1 unit of DNase I at 37°C for 1 h to destroy free viral DNA, followed by a heat inactivation step at 70°C for 10 min. Proteinase K was then added at a concentration of 0.1 mg/ml for 1 h at 50°C and heat inactivated at 75°C for 20 min. Aliquots were diluted 1/10 with water and amplified by qPCR using primers and probes specific to the BALF5 DNA polymerase gene and a TaqMan universal mastermix as previously described (47). A standard curve was used to calculate EBV copy numbers per ml.

Virus infections. B cells purified from peripheral blood with CD19-specific antibodies were exposed to viral supernatant for 2 h at a multiplicity of infection (MOI) of 10 viral genomes per B cell, then washed once with PBS and cultured with RPMI supplemented with 20% FBS in the absence of immunosuppressive drugs. Three days after infection, an EBNA2 staining was performed, 3 EBNA2-positive B cells per well were seeded into 48 wells of 96-well U-bottomed plates that contained 10^3 gamma-irradiated NHDF

feeder cells. We included noninfected B cells as a negative control. Outgrowth of lymphoblastoid cell clones was monitored for 30 days postinfection. Viruses used for infection of primary epithelial cells or of NSG-A2 mice were obtained by ultracentrifugation of infectious supernatants (30,000 × *g* for 2 h at 4°C with a TLA-110 Beckman rotor) and resuspended in PBS. Transfer infection of primary epithelial cells was performed by coculture with primary B cells previously exposed to viral supernatants at an MOI of 100 for 2 h at room temperature and left in RPMI-20% FBS for 20 h in a CO_2 incubator (17). Virus-loaded B cells were then washed once in culture medium used for primary epithelial cells (KGM-SFM; Invitrogen) and cocultured with primary epithelial cells at a concentration of 3 virus-loaded B cells per epithelial cell. The B cells were carefully removed 24 h postseeding, and the infection rate of the primary epithelial cells was determined 48 h thereafter by *in situ* hybridization with an EBER-specific peptide nucleic acid (PNA) probe in conjunction with a PNA ISH detection kit (Dako) according to the manufacturers' protocols.

Transformation experiments in nonhumanized NSG mice. We isolated human $CD19^+$ B cells from buffy coats and exposed them to virus supernatants at a multiplicity of infection sufficient to generate 20% EBNA2-positive cells for 2 h at room temperature under constant agitation (18). The infected cells were collected by centrifugation and washed twice with PBS. An aliquot of 2×10^6 of these cells, equivalent to 4×10^5 infected cells, was injected intraperitoneally into NSG mice (18). The mice were euthanized at 5 weeks postinjection and autopsied, and their organs were subjected to macroscopic and microscopic investigation.

Immunohistochemistry. Organs from the euthanized NSG mice were fixed in 10% formalin and embedded in paraffin, and 3-μm thin sections were prepared and immunostained after antigen retrieval (10 mM sodium citrate and 0.05% Tween 20 [pH 6.0] at 99°C for 45 min). Bound antibodies were visualized with the Envision+ Dual link system-horseradish peroxidase (HRP) (Dako). Pictures were taken with a camera attached to a light microscope (DM2500; Leica). Measurements on stained tissues were performed with Leica Suite X software. Paired Student's *t* tests were performed with GraphPad Prism 8.0 to assess the statistical significance of the results.

Chemical inducers and calcium signaling. Aliquots of 1×10^5 cells from the panel of spontaneous LCLs and of B cells transformed by rB95-8, rM81, or rMSHJ were seeded into one well of a 96-well plate and incubated for 3 days with ionomycin (1 μg/ml), TPA (20 ng/ml)-butyrate (3.3 mM), or TGF-β (0.5 ng/ml). In another set of experiments, cells were treated with cyclosporine (CSA; 1 μg/ml), with anti-human B-cell receptor antibodies [IgG/A/M (H+L) $F(ab')_2$ fragment, 20 μg/ml (Sigma)], rapamycin (10 mM), or ibrutinib (10 nM and 100 nM) for 7 days. A 10 nM concentration of ibrutinib fully inactivates the Btk active site (19). After 7 days, an immunofluorescent staining for BZLF1 was performed, and the number of positive cells was determined by counting. The experiment was performed in triplicate and included mock-treated cells as a control.

Cell lines. HEK293 is a neuroendocrine cell line obtained by transformation of embryonic epithelial kidney cells with adenovirus (48). Peripheral blood $CD19^+$ B cells were isolated from fresh buffy coats by Ficoll density gradient followed by selection with anti-CD19 PanB Dynabeads and detachment of the beads, as recommended by the manufacturer (Invitrogen). These cells were exposed to various viruses to generate new virus-transformed cell lines (daughter cells). LCLs and cell lines were routinely cultured in RPMI 1640 medium (Invitrogen) supplemented with 10% fetal bovine serum (FBS; Biochrom).

Hypoxia treatment. Aliquots of 1×10^5 cells from the rB95-8, rM81, and rMSHJ cell lines were seeded into one well of a 96-well plate and maintained under hypoxic conditions (1.0% O_2) in an InvivO2 workstation (Baker) for 1, 3, 5, or 7 days. Cells kept under nonhypoxic atmospheric O_2 concentrations (5% CO_2) served as a control. The experiment was performed in triplicate at 35 and 90 days postinfection.

Data availability. The sequences of the MSHJ and IM-3 genomes are available in GenBank under accession numbers MK973062 and MK973061.

ACKNOWLEDGMENTS

We thank the staff of the DKFZ animal facility, the High Throughput Sequencing Unit, the Central Unit for Electron Microscopy, and the Imaging and Cytometry Core Facility at DKFZ for excellent technical support.

Ming-Han Tsai is supported by the Ministry of Science and Technology, Taiwan (grant MOST-108-2636-B-010-001). Susanne Delecluse was supported by a maternity leave from the DZIF.

REFERENCES

1. Rickinson AB, Kieff E. 2007. Epstein-Barr virus, p 2655–2700. *In* Knipe DM, Howley PM, Griffin DE, Lamb RA, Martin MA, Roizman B, Strauss SE (ed). Lippincott Williams & Wilkins, Philadelphia, PA.
2. Dolcetti R, Dal Col J, Martorelli D, Carbone A, Klein E. 2013. Interplay among viral antigens, cellular pathways and tumor microenvironment in the pathogenesis of EBV-driven lymphomas. Semin Cancer Biol 23:441–456. https://doi.org/10.1016/j.semcancer.2013.07.005.
3. Klinke O, Feederle R, Delecluse HJ. 2014. Genetics of Epstein-Barr virus microRNAs. Semin Cancer Biol 26:52–59. https://doi.org/10.1016/j.semcancer.2014.02.002.
4. Tsai M-H, Raykova A, Klinke O, Bernhardt K, Gärtner K, Leung CS, Geletneky K, Sertel S, Münz C, Feederle R, Delecluse H-J. 2013. Spontaneous lytic replication and epitheliotropism define an Epstein-Barr virus strain found in carcinomas. Cell Rep 5:458–470. https://doi.org/10.1016/j.celrep.2013.09.012.
5. Coghill AE, Hildesheim A. 2014. Epstein-Barr virus antibodies and the risk of associated malignancies: review of the literature. Am J Epidemiol 180:687–695. https://doi.org/10.1093/aje/kwu176.
6. Chien YC, Chen JY, Liu MY, Yang HI, Hsu MM, Chen CJ, Yang CS. 2001. Serologic markers of Epstein-Barr virus infection and nasopharyngeal carcinoma in Taiwanese men. N Engl J Med 345:1877–1882. https://doi.org/10.1056/NEJMoa011610.

7. Montone KT, Hodinka RL, Salhany KE, Lavi E, Rostami A, Tomaszewski JE. 1996. Identification of Epstein-Barr virus lytic activity in post-transplantation lymphoproliferative disease. Mod Pathol 9:621–630.
8. Rea D, Delecluse HJ, Hamilton-Dutoit SJ, Marelle L, Joab I, Edelman L, Finet JF, Raphael M, French Study Group of Pathology for HIV-associated Tumors.1994. Epstein-Barr virus latent and replicative gene expression in post-transplant lymphoproliferative disorders and AIDS-related non-Hodgkin's lymphomas. Ann Oncol 5(Suppl 1):113–116.
9. Shumilov A, Tsai MH, Schlosser YT, Kratz AS, Bernhardt K, Fink S, Mizani T, Lin X, Jauch A, Mautner J, Kopp-Schneider A, Feederle R, Hoffmann I, Delecluse HJ. 2017. Epstein-Barr virus particles induce centrosome amplification and chromosomal instability. Nat Commun 8:14257. https://doi.org/10.1038/ncomms14257.
10. Delecluse S, Yu J, Bernhardt K, Haar J, Poirey R, Tsai MH, Kiblawi R, Kopp-Schneider A, Schnitzler P, Zeier M, Dreger P, Wuchter P, Bulut OC, Behrends U, Delecluse HJ. 2019. Spontaneous lymphoblastoid cell lines from patients with Epstein-Barr virus infection show highly variable proliferation characteristics that correlate with the expression levels of viral microRNAs. PLoS One 14:e0222847. https://doi.org/10.1371/journal.pone.0222847.
11. McKenzie J, El-Guindy A. 2015. Epstein-Barr virus lytic cycle reactivation. Curr Top Microbiol Immunol 391:237–261. https://doi.org/10.1007/978-3-319-22834-1_8.
12. Gutierrez MI, Ibrahim MM, Dale JK, Greiner TC, Straus SE, Bhatia K. 2002. Discrete alterations in the BZLF1 promoter in tumor and non-tumor-associated Epstein-Barr virus. J Natl Cancer Inst 94:1757–1763. https://doi.org/10.1093/jnci/94.23.1757.
13. Bristol JA, Djavadian R, Albright ER, Coleman CB, Ohashi M, Hayes M, Romero-Masters JC, Barlow EA, Farrell PJ, Rochford R, Kalejta RF, Johannsen EC, Kenney SC. 2018. A cancer-associated Epstein-Barr virus BZLF1 promoter variant enhances lytic infection. PLoS Pathog 14:e1007179. https://doi.org/10.1371/journal.ppat.1007179.
14. Palser AL, Grayson NE, White RE, Corton C, Correia S, Ba Abdullah MM, Watson SJ, Cotten M, Arrand JR, Murray PG, Allday MJ, Rickinson AB, Young LS, Farrell PJ, Kellam P. 2015. Genome diversity of Epstein-Barr virus from multiple tumor types and normal infection. J Virol 89:5222–5237. https://doi.org/10.1128/JVI.03614-14.
15. Gratama JW, Oosterveer MA, Weimar W, Sintnicolaas K, Sizoo W, Bolhuis RL, Ernberg I. 1994. Detection of multiple 'Ebnotypes' in individual Epstein-Barr virus carriers following lymphocyte transformation by virus derived from peripheral blood and oropharynx. J Gen Virol 75:85–94. https://doi.org/10.1099/0022-1317-75-1-85.
16. Feederle R, Neuhierl B, Bannert H, Geletneky K, Shannon-Lowe C, Delecluse HJ. 2007. Epstein-Barr virus B95.8 produced in 293 cells shows marked tropism for differentiated primary epithelial cells and reveals interindividual variation in susceptibility to viral infection. Int J Cancer 121:588–594. https://doi.org/10.1002/ijc.22727.
17. Shannon-Lowe CD, Neuhierl B, Baldwin G, Rickinson AB, Delecluse HJ. 2006. Resting B cells as a transfer vehicle for Epstein-Barr virus infection of epithelial cells. Proc Natl Acad Sci U S A 103:7065–7070. https://doi.org/10.1073/pnas.0510512103.
18. Lin X, Tsai MH, Shumilov A, Poirey R, Bannert H, Middeldorp JM, Feederle R, Delecluse HJ. 2015. The Epstein-Barr virus BART miRNA cluster of the M81 strain modulates multiple functions in primary B cells. PLoS Pathog 11:e1005344. https://doi.org/10.1371/journal.ppat.1005344.
19. Brown JR. 2013. Ibrutinib (PCI-32765), the first BTK (Bruton's tyrosine kinase) inhibitor in clinical trials. Curr Hematol Malig Rep 8:1–6. https://doi.org/10.1007/s11899-012-0147-9.
20. Kosowicz JG, Lee J, Peiffer B, Guo Z, Chen J, Liao G, Hayward SD, Liu JO, Ambinder RF. 2017. Drug modulators of B cell signaling pathways and Epstein-Barr virus lytic activation. J Virol 91:e00747-17. https://doi.org/10.1128/JVI.00747-17.
21. Adamson AL, Le BT, Siedenburg BD. 2014. Inhibition of mTORC1 inhibits lytic replication of Epstein-Barr virus in a cell-type specific manner. Virol J 11:110. https://doi.org/10.1186/1743-422X-11-110.
22. Kraus RJ, Yu X, Cordes BA, Sathiamoorthi S, Iempridee T, Nawandar DM, Ma S, Romero-Masters JC, McChesney KG, Lin Z, Makielski KR, Lee DL, Lambert PF, Johannsen EC, Kenney SC, Mertz JE. 2017. Hypoxia-inducible factor-1α plays roles in Epstein-Barr virus's natural life cycle and tumorigenesis by inducing lytic infection through direct binding to the immediate-early *BZLF1* gene promoter. PLoS Pathog 13:e1006404. https://doi.org/10.1371/journal.ppat.1006404.
23. Lucker A, Weber B, Jenny P. 2015. A dynamic model of oxygen transport from capillaries to tissue with moving red blood cells. Am J Physiol Heart Circ Physiol 308:H206–H216. https://doi.org/10.1152/ajpheart.00447.2014.
24. Fina L, Molgaard HV, Robertson D, Bradley NJ, Monaghan P, Delia D, Sutherland DR, Baker MA, Greaves MF. 1990. Expression of the CD34 gene in vascular endothelial cells. Blood 75:2417–2426. https://doi.org/10.1182/blood.V75.12.2417.2417.
25. Miller G, Robinson J, Heston L, Lipman M. 1974. Differences between laboratory strains of Epstein-Barr virus based on immortalization, abortive infection, and interference. Proc Natl Acad Sci U S A 71:4006–4010. https://doi.org/10.1073/pnas.71.10.4006.
26. Davies ML, Xu S, Lyons-Weiler J, Rosendorff A, Webber SA, Wasil LR, Metes D, Rowe DT. 2010. Cellular factors associated with latency and spontaneous Epstein-Barr virus reactivation in B-lymphoblastoid cell lines. Virology 400:53–67. https://doi.org/10.1016/j.virol.2010.01.002.
27. Sculley TB, Moss DJ, Hazelton RA, Pope JH. 1987. Detection of Epstein-Barr virus strain variants in lymphoblastoid cell lines 'spontaneously' derived from patients with rheumatoid arthritis, infectious mononucleosis and normal controls. J Gen Virol 68:2069–2078. https://doi.org/10.1099/0022-1317-68-8-2069.
28. Babcock GJ, Decker LL, Freeman RB, Thorley-Lawson DA. 1999. Epstein-Barr virus-infected resting memory B cells, not proliferating lymphoblasts, accumulate in the peripheral blood of immunosuppressed patients. J Exp Med 190:567–576. https://doi.org/10.1084/jem.190.4.567.
29. Qu L, Green M, Webber S, Reyes J, Ellis D, Rowe D. 2000. Epstein-Barr virus gene expression in the peripheral blood of transplant recipients with persistent circulating virus loads. J Infect Dis 182:1013–1021. https://doi.org/10.1086/315828.
30. Hopwood PA, Brooks L, Parratt R, Hunt BJ, Bokhari M, Thomas JA, Yacoub M, Crawford DH, Maria B, Alero TJ, Magdi Y. 2002. Persistent Epstein-Barr virus infection: unrestricted latent and lytic viral gene expression in healthy immunosuppressed transplant recipients. Transplantation 74:194–202. https://doi.org/10.1097/00007890-200207270-00009.
31. Burns DM, Tierney R, Shannon-Lowe C, Croudace J, Inman C, Abbotts B, Nagra S, Fox CP, Chaganti S, Craddock CF, Moss P, Rickinson AB, Rowe M, Bell AI. 2015. Memory B-cell reconstitution following allogeneic hematopoietic stem cell transplantation is an EBV-associated transformation event. Blood 126:2665–2675. https://doi.org/10.1182/blood-2015-08-665000.
32. Fink S, Tsai MH, Schnitzler P, Zeier M, Dreger P, Wuchter P, Bulut OC, Behrends U, Delecluse HJ. 2017. The Epstein-Barr virus DNA load in the peripheral blood of transplant recipients does not accurately reflect the burden of infected cells. Transpl Int 30:57–67. https://doi.org/10.1111/tri.12871.
33. Buck M, Cross S, Krauer K, Kienzle N, Sculley TB. 1999. A-type and B-type Epstein-Barr virus differ in their ability to spontaneously enter the lytic cycle. J Gen Virol 80:441–445. https://doi.org/10.1099/0022-1317-80-2-441.
34. Vakiani E, Nandula SV, Subramaniyam S, Keller CE, Alobeid B, Murty VV, Bhagat G. 2007. Cytogenetic analysis of B-cell posttransplant lymphoproliferations validates the World Health Organization classification and suggests inclusion of florid follicular hyperplasia as a precursor lesion. Hum Pathol 38:315–325. https://doi.org/10.1016/j.humpath.2006.08.014.
35. Bhende PM, Seaman WT, Delecluse HJ, Kenney SC. 2005. BZLF1 activation of the methylated form of the *BRLF1* immediate-early promoter is regulated by BZLF1 residue 186. J Virol 79:7338–7348. https://doi.org/10.1128/JVI.79.12.7338-7348.2005.
36. Weiss ER, Lamers SL, Henderson JL, Melnikov A, Somasundaran M, Garber M, Selin L, Nusbaum C, Luzuriaga K. 2018. Early Epstein-Barr virus genomic diversity and convergence toward the B95.8 genome in primary infection. J Virol 92. https://doi.org/10.1128/JVI.01466-17.
37. Li Z, Tsai MH, Shumilov A, Baccianti F, Tsao SW, Poirey R, Delecluse HJ. 2019. Epstein-Barr virus ncRNA from a nasopharyngeal carcinoma induces an inflammatory response that promotes virus production. Nat Microbiol 4:2475–2486. https://doi.org/10.1038/s41564-019-0546-y.
38. Desgranges C, Lenoir G, de-The G, Seigneurin JM, Hilgers J, Dubouch P. 1976. *In vitro* transforming activity of EBV. I. Establishment and properties of two EBV strains (M81 and M72) produced by immortalized *Callithrix jacchus* lymphocytes. Biomedicine 25:349–352.
39. Miller G, Shope T, Lisco H, Stitt D, Lipman M. 1972. Epstein-Barr virus: transformation, cytopathic changes, and viral antigens in squirrel monkey and marmoset leukocytes. Proc Natl Acad Sci U S A 69:383–387. https://doi.org/10.1073/pnas.69.2.383.

40. Pulvertaft JV. 1964. Cytology of Burkitt's tumour (African lymphoma). Lancet 1:238–240. https://doi.org/10.1016/S0140-6736(64)92345-1.
41. Griffin BE, Bjorck E, Bjursell G, Lindahl T. 1981. Sequence complexity of circular Epstein-Bar virus DNA in transformed cells. J Virol 40:11–19. https://doi.org/10.1128/JVI.40.1.11-19.1981.
42. Katoh K, Misawa K, Kuma K, Miyata T. 2002. MAFFT: a novel method for rapid multiple sequence alignment based on fast Fourier transform. Nucleic Acids Res 30:3059–3066. https://doi.org/10.1093/nar/gkf436.
43. Gardella T, Medveczky P, Sairenji T, Mulder C. 1984. Detection of circular and linear herpesvirus DNA molecules in mammalian cells by gel electrophoresis. J Virol 50:248–254. https://doi.org/10.1128/JVI.50.1.248-254.1984.
44. Delecluse HJ, Hilsendegen T, Pich D, Zeidler R, Hammerschmidt W. 1998. Propagation and recovery of intact, infectious Epstein-Barr virus from prokaryotic to human cells. Proc Natl Acad Sci U S A 95:8245–8250. https://doi.org/10.1073/pnas.95.14.8245.
45. Neuhierl B, Feederle R, Hammerschmidt W, Delecluse HJ. 2002. Glycoprotein gp110 of Epstein-Barr virus determines viral tropism and efficiency of infection. Proc Natl Acad Sci U S A 99:15036–15041. https://doi.org/10.1073/pnas.232381299.
46. Granato M, Feederle R, Farina A, Gonnella R, Santarelli R, Hub B, Faggioni A, Delecluse HJ. 2008. Deletion of Epstein-Barr virus BFLF2 leads to impaired viral DNA packaging and primary egress as well as to the production of defective viral particles. J Virol 82:4042–4051. https://doi.org/10.1128/JVI.02436-07.
47. Feederle R, Bannert H, Lips H, Muller-Lantzsch N, Delecluse HJ. 2009. The Epstein-Barr virus alkaline exonuclease BGLF5 serves pleiotropic functions in virus replication. J Virol 83:4952–4962. https://doi.org/10.1128/JVI.00170-09.
48. Shaw G, Morse S, Ararat M, Graham FL. 2002. Preferential transformation of human neuronal cells by human adenoviruses and the origin of HEK 293 cells. FASEB J 16:869–871. https://doi.org/10.1096/fj.01-0995fje.